Doppler backscattering measurements for MAST

J.C. Hillesheim[1,2], W.A. Peebles[3], H.F. Meyer[1], N.A. Crocker[3], and the MAST Team[1]

[1] *EURATOM/CCFE Fusion Association, Abingdon, Oxon, OX14 3DB, UK*

[2] *Rudolph Peierls Centre for Theoretical Physics, University of Oxford, Oxford, OX1 3NP, UK*

[3] *University of California, Los Angeles, Los Angeles, California 90095-7099, USA*

Turbulent transport of particles, heat, and momentum continues to be an active area of research in the pursuit of fusion energy through magnetically confined plasmas. Doppler backscattering [1, 2] (DBS) has become a well-established and versatile diagnostic technique for the measurement of intermediate-k ($k_\theta \rho_s \sim 1$) density fluctuations and flows in magnetically confined fusion experiments. In this paper we discuss the impact of general considerations for the scattering of electromagnetic radiation from plasma density fluctuations on the DBS technique, in particular the dependence of scattered power on scattering alignment. We use this approach for the optimization of DBS for the MAST [3] spherical tokamak. Two 8-channel millimeter-wave diagnostic systems [8] were installed on NSTX for use as reflectometers. One system operates mostly within Q-band, with frequencies spanning 30-50 GHz. The second operates in V-band, covering 55-75 GHz. With NSTX under construction for an upgrade during 2013, an equipment transfer through a collaboration between MAST and UCLA has been undertaken to install the two systems on MAST for the 2013 experimental campaign, with the capability to function either as conventional reflectometers or for Doppler backscattering.

In the limit where the electromagnetic wave frequency is much larger than the plasma frequency and electron cyclotron frequency, $\omega >> \omega_{pe},\ \omega_{ce}$, the Born approximation can be used to calculate the scattered electric field for a beam incident on a volume of plasma with density fluctuations [4]. This limit is not well satisfied for DBS, where refraction of the probe beam is fundamental to the technique; however, the same basic concepts apply for wave-vector matching in both techniques. These considerations limit the accuracy of simplified analytical results.

It can be shown that (neglecting relativistic effects) the electric field scattered by plasma density fluctuations follows [4, 5]

$$\mathbf{E_s}(\omega_s) = \left[\hat{\mathbf{k}}_s \times \left(\hat{\mathbf{k}}_s \times \mathbf{E_0}\right)\right] \frac{r_0}{16\pi^4\sqrt{a_x a_y}} \int d\omega_n dt d\mathbf{k}_n d\mathbf{x} \qquad (1)$$
$$\widetilde{n}(\mathbf{k_n}, \omega_n) e^{-x^2/a_x^2} e^{-y^2/a_y^2} e^{-i(\omega_i+\omega_n-\omega_s)t} e^{i(\mathbf{k}_i+\mathbf{k}_n-\mathbf{k}_s)\mathbf{x}} e^{-i\omega_s R/c} + \text{c.c.}$$

Here x and y are the directions transverse to the propagation of the beam and z is along the axis of the beam. $\mathbf{E_0}$ is the incident electric field and $\widetilde{n}(\mathbf{k_n}, \omega_n)$ is the spectrum of density fluctuations. We have assumed a Gaussian beam with beam widths a_x and a_y, which vary along z. The classical electron radius is $r_0 = e^2/4\pi\varepsilon_0 m_e c^2$. The indices $j = n, i, s$ for the wave-vector and frequency are for the density fluctuations, incident radiation, and scattered radiation, respectively; R is the distance the scattered radiation travels to the detector.

Equation 1 can be reduced to isolate the effect of interest, the dependence of scattered power along the path on scattering alignment [6]. For simplicity, take $a_x = a_y = a_0$. Define θ_{mis} as the mismatch angle, $\hat{\mathbf{k}}_s \cdot \hat{\mathbf{B}} = \cos(\pi/2 - \theta_{mis})$, so that scattered power is maximal for $\theta_{mis} = 0$ (assuming a monostatic antenna arrangment); then, $k_{s,x} = |\mathbf{k_s}| \sin\theta_{mis}$. Equation 1 is then (assuming fluctuations are elongated along field lines, $k_{s,x} >> k_{n,x}$)

$$dI \propto dz\, \widetilde{n}^2(\mathbf{k_n}, z) \exp\left(-\frac{|\mathbf{k}_s|^2 a_0^2 \sin^2\theta_{mis}}{2}\right). \tag{2}$$

For small θ_{mis} $\sin\theta_{mis} \approx \theta_{mis}$ and $|\mathbf{k}_s| \approx |\mathbf{k}_n|/2$ (i.e. for small θ_{mis}, $|\mathbf{k}_s| \approx k_{s,\perp}$). In terms of the scattering wavenumber of density fluctuations, we arrive at a criterion that for significant scattered power (taken to be $1/e$):

$$|\theta_{mis}| \lesssim \frac{2\sqrt{2}}{k_n a_0}. \tag{3}$$

This provides a rough rule-of-thumb for design considerations.

Density profiles and magnetic equilibria for MAST have been surveyed to assess profile access. During low density L-mode periods, the Q-band system is expected to provide coverage of most of the inner radius, typically covering from near the edge to $r/a \sim 0.5$. This is ideal for core turbulence studies when used for either reflectometry or DBS, and for L-H transition studies. The V-band system is expected to either not encounter a cutoff or encounter one deep in the core plasma in L-mode. This will enable fast ion mode studies in MAST. In H-mode plasmas, the Q-band system will access the lower two-thirds to half of the pedestal, while the V-band system will access the top of the pedestal, and possibly the core locations, depending on details of the density profile and which polarization is used.

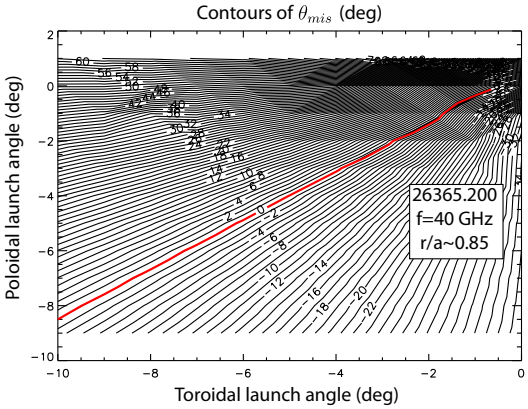

Figure 1: Contours of θ_{mis} at the ray turning point as a function of poloidal and toroidal launch angle. Launch frequency is 40 GHz in X-mode during an L-mode portion of a MAST shot. The optimal condition of $\theta_{mis} = 0^\circ$ is plotted in red.

Ray tracing using the Genray code [7] has been implemented for MAST, using experimental equilibrium and density information. The Appleton-Hartree (cold plasma) dispersion relation is used. Ray tracing is used to calculate the θ_{mis} parameter to assess several design and implementation considerations.

Figure 1 shows the result of calculating θ_{mis} at the ray turning point (minimum perpendicular index of refraction along the ray) as a function of toroidal and poloidal angle, originating from the MAST port window to be used for the DBS implementation. The plasma chosen in this example is in L-mode and the launch frequency of 40 GHz in X-mode polarization approaches cutoff at $r/a \approx 0.85$. The optimal launch condition of $\theta_{mis} = 0^\circ$ is plotted in red. Although the

corresponding wavenumbers are not included in the plot, the calculations project that about 10° steering will enable measurements of $k_{n,\perp} \sim 4-12$ cm^{-1}. With the relatively low magnetic field in MAST (~ 0.5 T), this corresponds to $k_{n,\perp}\rho_s \sim 2-7$. One can also see from the plot that accurate beam steering is essential. Using Eqn. 3 for an estimate and assuming $a_0 \approx 4$ cm, one finds for higher wavenumbers at fixed poloidal angle, the toroidal launch angle must be accurate to within $\sim \pm 1°$, while for lower wavenumbers the launch must still be accurate to within $\sim \pm 2°$. Experimental validation of these calculations will be a high priority soon after the system is installed.

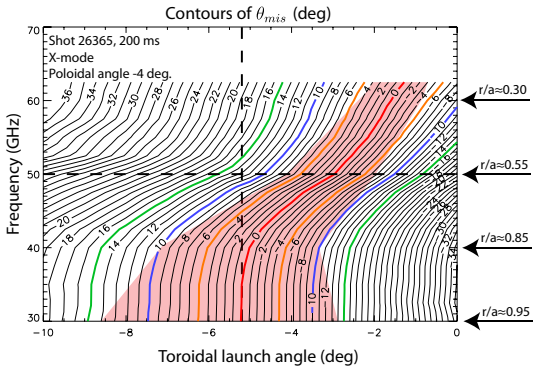

Figure 2: Ray tracing results showing contours of θ_{mis} (at the ray turning point) as a function of frequency and toroidal launch angle for an L-mode MAST plasma at a fixed poloidal angle of $-4°$. Contours colored and dashed lines added for ease of viewing. Shaded area approximately indicates where $|\theta_{mis}| < 2\sqrt{2}/(k_n a_0)$, assuming $a_0 = 4$ cm.

An example of the dependence of θ_{mis} at the ray turning point on launch frequency and toroidal launch angle is illustrated in Fig. 2. This calculation is of particular interest since the launched frequencies would effectively be a vertical cut through such a plot. Note the calculation is for X-mode only and would apply either for 50 GHz and below for the Q-band system, or above for the V-band system; a similar plot would exist for O-mode. For frequencies of 30, 40, 50, and 60 GHz the respective scattering locations would be $r/a \sim$0.95, 0.85, 0.55, and 0.30, while the scattering wavenumbers would be $k_{n,\perp} \sim 3$, 4, 6, and 10 cm^{-1}. The allowable misalignment from Eqn. 3, assuming $a_0 \approx 4$ cm, would then be about 14°, 10°, 7°, and 4°. Due to changes in pitch angle and narrowing of the allowable mismatch, the number of channels that can be simultaneously aligned is projected to be limited. However, little signal is often observed with DBS measurements deep in the core ($r/a \lesssim 0.5$), even in standard tokamaks. The calculations do project that in many cases 1/3 to 1/2 of the minor radius will simultaneously be within reasonable alignment for L-mode portions of shots. Pedestal measurements in H-mode plasmas should not be greatly impacted, due to their close spatial proximity.

An additional challenge for implementation in MAST is the relatively short plasma duration, ~ 0.5 s. Diffusion does not have sufficient time to relax the current profile to a steady-state. This results in a continuously evolving safety factor profile, which directly impacts magnetic field pitch angle and therefore scattering alignment. Figure 3 shows the evolution of misalignment angle at the turning point over time, along with the scattering wavenumber and location. Also plotted are the plasma current, density, and safety factor at the edge and on axis. Horizontal lines have been added to Fig. 3(a) for reference at 0°, $\pm 5°$, and 10°. One can see that there is over 150 ms time period where all frequencies are aligned to within $|\theta_{mis}| < 10°$, with over 100 ms where $|\theta_{mis}| < 5°$ for all channels. This shows that the outer $\sim 1/3$ of the plasma should be able

to be accessed simultaneously towards the end of the discharge. The effect of scanning toroidal launch angle is essentially to move results as in Fig. 3(a) up or down in θ_{mis}. If desired, it should also be possible to target a window earlier in the shot for alignment, rather than optimizing for when the current profile is approaching a relaxed steady-state, as pictured.

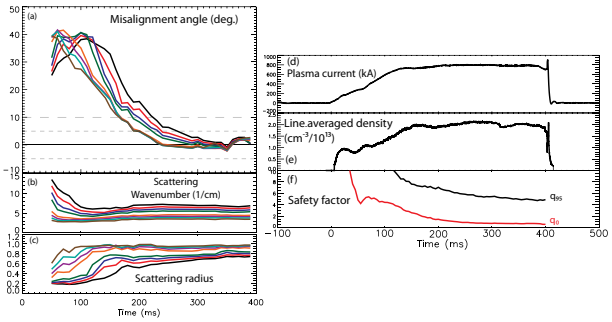

Figure 3: Ray tracing results for a poloidal launch angle of -4° and toroidal launch angle of -6° in an L-mode MAST plasma as a function of time showing (a) the misalignment angle at the turning point, (b) scattering wavenumber, and (c) scattering normalized minor radius. Q-band system frequencies, 30-50 GHz, launched in X-mode. Also plotted are the (d) plasma current, (e) line averaged density, (f) and safety factor at the edge and on axis.

In this paper, plans for the implementation of DBS and reflectometry in MAST have been discussed. We found that the planned implementation of DBS/reflectometry on MAST, through the temporary equipment transfer from NSTX should provide measurements in a wide range of plasma conditions. The mechanical implementation to realize this set of calculations will be accomplished with a quasi-optical beam system, where a polarizer is used to combine the beam path of the two systems, and a remotely controllable mirror allows the launched beam to be steered both toroidally and poloidally. Initial plans following implementation will be confirming presented calculations by varying expected alignment. The diagnostics will then be used to support physics goals of MAST experiments.

Acknowledgements

This work was funded by the RCUK Energy Programme [grant number EP/I501045], the European Communities under the contract of Association between EURATOM and CCFE, and the US Department of Energy under DE-FG02-99ER54527. The views and opinions expressed herein do not necessarily reflect those of the European Commission.

References

[1] E. Holzhauer *et al.*, Plasma Phys. Controlled Fusion **40** 1869 (1998).
[2] M. Hirsch *et al.*, Plasma Phys. Controlled Fusion **43** 1641 (2001).
[3] B. Lloyd *et al.*, Nucl. Fusion **43**, 1665 (2003).
[4] G. Bekefi, *Radiation Processes in Plasmas*, 1st Ed. (Wiley, 1966).
[5] R.E. Slusher and C.M. Surko, Physics of Fluids **23**, 472 (1980).
[6] J.C. Hillesheim *et al. Proc.* 11th *Intl. Reflectometry Workshop - IRW11* (2013).
[7] A.P. Smirnov and R.W. Harvey, Bull. Am. Phys. Soc. **40**, 1837 (1995).
[8] N.A. Crocker *et al.*, Plasma Phys. Controlled Fusion **53**, 105001 (2011).